J Appl Electrochem (2007) 37:653–660
DOI 10.1007/s10800-007-9314-4

ORIGINAL PAPER

Electrochemical oxidation of alcoholamines at gold

Teresa Łuczak

Received: 18 December 2006 / Accepted: 14 January 2007 / Published online: 10 March 2007

Abstract Gold is a good electrocatalyst for alcoholamine oxidation in basic media. In this work the effect of alcoholamine concentration, electrolyte pH and potential scan rate on electrooxidation was studied. The adsorption of alcoholamines on a $\mathrm{AuOH}_{\mathrm{ad}}^{\delta-}$ layer plays a significant role in the oxidation mechanism. The rate determining step of the process was found to be heterogeneous dehydrogenation of the alcoholamine molecule, involving electron transfer to the gold electrode and the formation of water molecule. The catalytic effect of the gold electrode on alcoholamine oxidation is higher than that observed both for aliphatic alcohol and amines.

Keywords Aliphatic alcoholamines · Electrooxidation · Electrocatalysis · Gold electrode · Adsorption

1 Introduction

The catalytic activity of noble metals for the electrooxidation of organic substances has been the subject of many studies. From among these metals gold and platinum are the most active and most often used electrocatalysts. Gold stands out because of its good electrocatalytic activity in alkaline environments [1–13], whereas platinum is the most active in acid [1, 2, 14, 15]. Oxidation of organic substances at platinum is accompanied by a characteristic, though very undesirable, effect of surface blocking by strongly adsorbed intermediate species [15]. This effect does not apply to gold which has no vacancy in its d-bands and thus is characterized by relatively poor adsorption properties [4, 16–23] as compared with platinum. Though these adsorption properties of gold account for its weak catalytic activity in acid solution, in alkaline solutions, when hydroxide ions adsorb on the gold surface [3, 4, 12, 24–30], gold proves to be a more effective catalyst for dehydrogenation of organic compounds than platinum.

Aliphatic amines are an important and widely used class of organic compounds. They have been used as starting or intermediate agents in the production of various other chemical compounds such as polymers, corrosion inhibitors, pesticides and pharmaceuticals. In spite of the unquestionable significance of aliphatic amines in industrial, clinical and environmental applications their electrochemical performance has been poorly recognized. For platinum electrodes it has been established that the mechanism of oxidation of aliphatic amines depends on the electrode potential and leads to cyanide species becoming adsorbed on the electrode surface in acidic as well as in alkaline medium [31–36]. On gold, the simultaneous oxidation of ethylamine and gold oxide (AuO) formation in aqueous alkaline media has been observed [37–40]. Relationships between the adsorption properties and electrocatalytic oxidation of a homologous series of aliphatic amines ranging from methylamine to butylamine have been evaluated and discussed [41–45]. It has been argued that the overall electrooxidation rate is influenced by the strength of electrosorption. The effect of molecular structure on isomeric butylamines has been analyzed [46]. The oxidation of the isomer with the -NH_2 group attached to the first ordered carbon atom yields current densities about three times higher than those obtained for the isomer with the –NH_2 group linked to the secondary ordered carbon atom. The striking difference between the isomers, caused by the molecular structure, is clear.

T. Łuczak (✉)
Department of Chemistry, A. Mickiewicz University,
Grunwaldzka 6, PL-60-780 Poznań, Poland
e-mail: telucz@amu.edu.pl

In this work the electrochemical reactivity of alcoholamines on a gold electrode is studied. Qualitative information about the relative adsorptivities of the molecules investigated was obtained from measurements of the differential capacitance of the electrical double layer of the electrode/solution interface at various organic concentrations. Comparison of the electrochemical properties of alcoholamines with those obtained previously for simple aliphatic alcohols [4, 12] and amines [41–46] was made.

2 Experimental

The experimental setups used to record cyclic voltammograms (*j–E* curves) and differential capacitance of the electric double layer versus electrode potential curves (*C–E*) are the same as those described earlier [6].

The electrochemical studies were carried out in a conventional three-compartment cell separated by glass frits. A gold bead (99.999% purity) of 0.3 cm^2 geometrical area and a gold sheet were used as working and auxiliary electrodes, respectively. A hydrogen electrode (RHE) in the supporting electrolyte as proposed by Will et al. [47, 48] was used as reference electrode. For comparison with published data all potentials in this paper are referred to the saturated calomel electrode (SCE).

The solutions were prepared from water purified in a Millipore Milli-Q system, 2-amino-1-ethanol (ethanolamine), 2-amino-1-butanol (butanolamine) from Aldrich and NaOH from Merck. All chemicals were analytical grade quality and were used as purchased without further purification. The solutions under investigation were deaerated with high purity argon before measurements. The measurements were performed at 295 K.

Prior to each series of measurements with alcoholamines, the working electrode was electrochemically activated by cycling ($dE/dt = 0.1$ V s^{-1}) in the potential range between $E = -1.1$ mV and $E = 0.15$ V versus SCE in the supporting electrolyte solution (0.1 mol dm^{-3} NaOH), where no faradaic reactions occur on the gold surface. This procedure avoids structural changes on the gold surface.

The *C–E* curves were obtained by superimposing an ac sinusoidal voltage signal (15 s^{-1}, 5 mV) on a slow linear electrode potential scan ($dE/dt = 0.005$ V s^{-1}). A slower scan rate of 0.002 V s^{-1} did not affect the *C–E* curves observed. The equilibrium of the adsorption/desorption was checked in additional experiments at different frequencies. For frequencies in the range 5–40 s^{-1} no frequency dispersion of the differential capacitance was observed in the potential range between –0.95 V and $E = 0.15$ V versus SCE, in the supporting electrolyte. This potential range narrows ($E = -0.35$ V–$E = 0.15$ V) in solutions containing both ethanolamine (in concentrations between 0.0001 and 0.5 mol dm^{-3}) and butanolamine (in concentrations between 0.0001 and 0.1 mol dm^{-3}). Stirring had no effect on the course of the *C–E* curves, which indicated that mass transport did not limit the rate of adsorption/desorption of alcoholamine at the bulk concentrations studied. Thus the differential capacity data in the above-mentioned potential range can be considered at equilibrium.

After each measurement with alcoholamines the working electrode was thoroughly rinsed with water and both *j–E* and *C–E* curves were recorded again in freshly prepared supporting electrolyte. Each time the shapes of the *j–E* and *C–E* curves were the same as those taken before the measurements. This means that the surface of the working gold electrode had not changed during the experiment with alcoholamines.

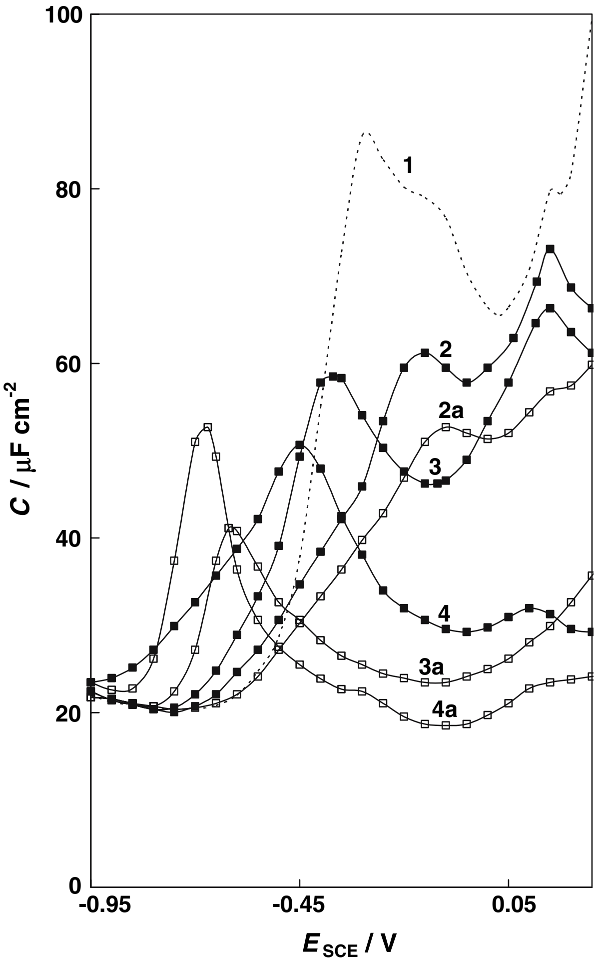

Fig. 1 Differential capacitance versus potential for the gold electrode in 0.1 mol dm^{-3} NaOH (curve 1) with increasing 2-aminoethanol (■) concentration: (2) 0.0001 mol dm^{-3}; (3) 0.001 mol dm^{-3}; (4) 0.01 mol dm^{-3} and with increasing 2-amino–1-butanol (□) concentration: (2a) 0.0001 mol dm^{-3}; (3a) 0.001 mol dm^{-3}; (4a) 0.01 mol dm^{-3}. $dE/dt = 0.005$ V s^{-1}

3 Results and discussion

Adsorption of the alcoholamines at the gold/solution interface is obvious from the results of differential capacitance of the electrical double layer measurements. The representative set of *C*–*E* curves illustrating changes in the differential capacitance as a function of electrode potential, in 0.1 mol dm^{-3} NaOH as a supporting electrolyte and at different concentrations of ethanolamine and butanolamine, is presented in Fig. 1. It should be noted that the potential range in which amine molecules are adsorbed on the gold/alkaline solution interface overlaps with that in which the adsorption of hydroxyl ions occurs. In the opinion of a number of authors the adsorbed hydroxyl ions participating in the oxidation of organics on gold are partly discharged according to the equation: $\mathrm{Au} + \mathrm{OH}^- \rightarrow \mathrm{AuOH}_{ad}^{\delta-} + (1 - \delta e)$ [2–5, 8, 12, 24–27, 49–51]. Because of the simultaneous competitive adsorption of organic molecules and OH$^-$ ions at the electrode a quantitative evaluation of the *C*–*E* curves is not possible and therefore, only qualitative information about the relative adsorptivity of the system can be attained. The suppression of the *C*–*E* curves with increasing bulk alcoholamine concentration takes place both in the potential range of the characteristic minimum in the vicinity of the potential of zero charge (E_{pzc}) of the gold electrode [41, 43] and in the adsorption/desorption maximum on the negatively charged surface. This observation gives clear evidence for the substitution of water with organic molecules at the gold surface. Relatively strong adsorption of alcoholamines on gold is manifested by the fact that the *C*–*E* curves for the highest solute concentration do not tend to coincide with the respective curve for the supporting electrolyte solution at about –0.9 V. This implies that some adsorbate molecules still remain at the electrode surface. The alcoholamine molecules are able to form surface complexes by coordinative interaction between the electrode surface and the electron lone pairs localized both at the nitrogen and oxygen atoms. Analysis of relationships of $\Theta = (C_{\Theta=0} - C_{\Theta})/(C_{\Theta=0} - C_{\Theta=1})$ versus c_A suggests increasingly stronger interaction of organic molecules with the gold electrode when passing from ethanolamine to butanolamine. The surface coverage for the same bulk alcoholamine concentration at chosen *E* is higher for compounds with longer carbon chain length in the

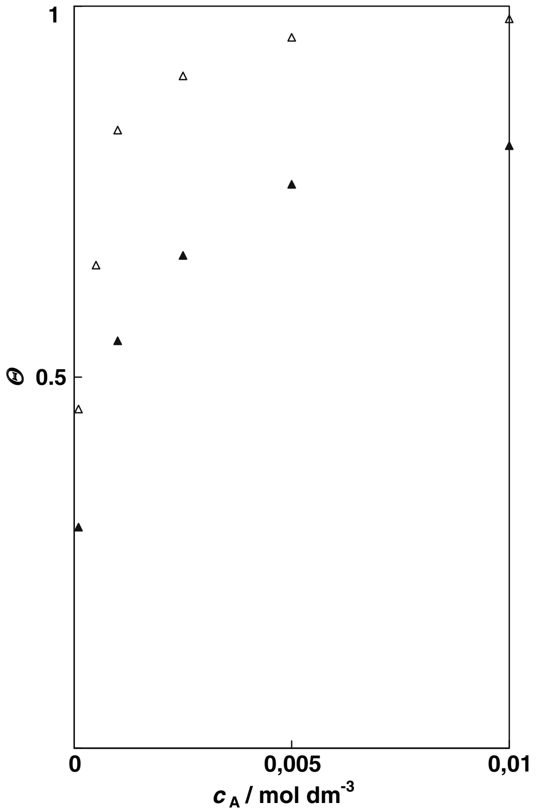

Fig. 2 Dependence of the gold electrode coverage on the amine concentrations in 0.1 mol dm^{-3} NaOH at E = –0.15 V versus SCE for (▲) 2-aminoethanol and (Δ) 2-amino–1-butanol. d*E*/d*t* = 0.005 V s^{-1}

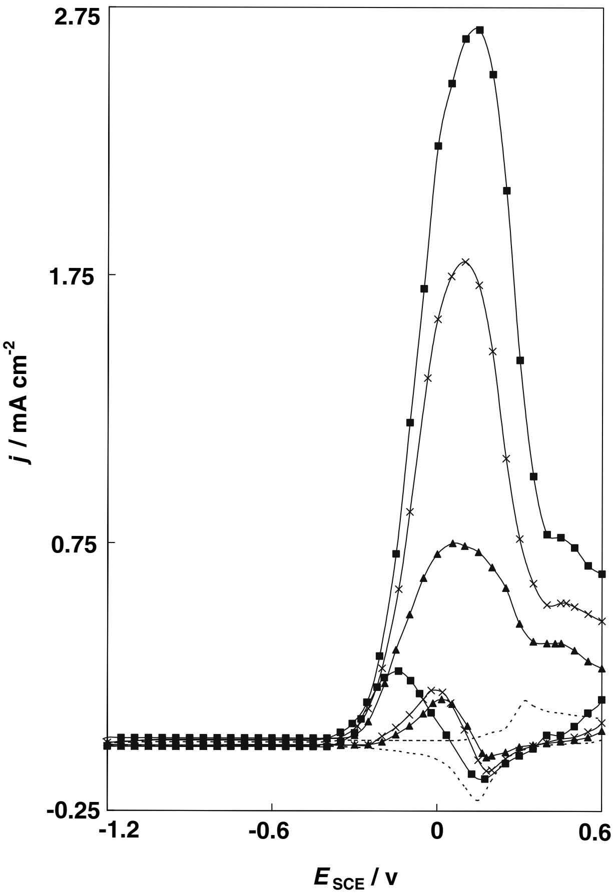

Fig. 3 Cyclic voltammograms of gold electrode in 0.1 mol dm^{-3} NaOH (dotted line) and with increasing concentration of 2-aminoethanol: (▲) 0.005 mol dm^{-3}; (×) 0.05 mol dm^{-3}; (■) 0.5 mol dm^{-3}. d*E*/d*t* = 0.1 V s^{-1}

alcoholamine molecule, Fig. 2. It should be emphasized that the concentration responsible for $\Theta = 1$ decreases with increasing carbon chain length in the alcoholamine molecule. The minimum differential capacitance ($C_{\Theta = 1}$) is reached in the case of butanolamine for the 5-fold smaller bulk solute concentration (0.1 mol dm^{-3}) than for ethanolamine (0.5 mol dm^{-3}).

The sets of cyclic voltammograms presented in Figs. 3 and 4 illustrate the electrooxidation activities of alcoholamines at gold in alkaline medium. For the sake of comparison the cyclic voltammogram of the bare electrode in the supporting electrolyte alone, 0.1 mol dm^{-3} NaOH, under the same experimental condition is included. A well-defined anodic peak at $E = 0.3$ V and a cathodic peak at $E = 0.14$ V visible in the j–E curve of the gold electrode are assigned to gold oxide formation and to its reduction, respectively [52]. The alcoholamine oxidation at the gold electrode proceeds irreversibly in the potential range in which coadsorption of organic molecules and OH^- ions occurs. This suggests that the hydroxyl ions play an important role in the mechanism. The oxidation of ethanolamine starts during the positive sweep above –0.35 V, Fig. 3, as observed by Johnson et al. [38]. An increase in the number of carbon atoms in the alcoholamine molecule results in the onset of electrooxidation moving negatively, e.g. the oxidation of butanolamine begins at about –0.55 V, Fig. 4. As the electrode potential becomes increasingly positive, well defined anodic peaks with maxima at $E \approx 0.06$ and 0.08 V appear on the cyclic voltammograms of ethanolamine and butanolamine of low bulk concentration (c_A), respectively. Alcoholamines are also oxidized in the potential region of gold oxide formation, although the rate of the process is much slower than in the potential region of hydroxyl ion adsorption. In the negative going sweep, oxidation takes place when the surface oxide layer begins to reduce reaching the maximum at $E \leq 0$ versus SCE.

For the alcoholamines studied a characteristic feature is an increase in the anodic current density with increasing concentration in the supporting electrolyte. (For clarity, not all j–E curves for the solute concentrations studied are presented.) In the positive scan of potential the maxima in the oxidation peaks shift positively when the bulk

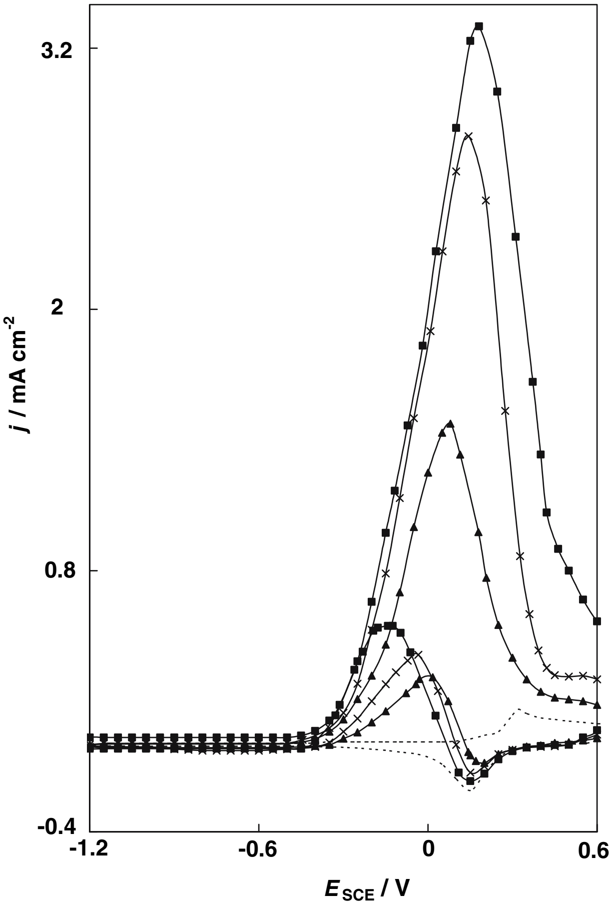

Fig. 4 Cyclic voltammograms of gold electrode in 0.1 mol dm^{-3} NaOH (dotted line) and with increasing concentration of 2-amino-1-butanol: (▲) 0.005 mol dm^{-3}; (×) 0.05 mol dm^{-3}; (■) 0.5 mol dm^{-3}. dE/dt = 0.1 V s^{-1}

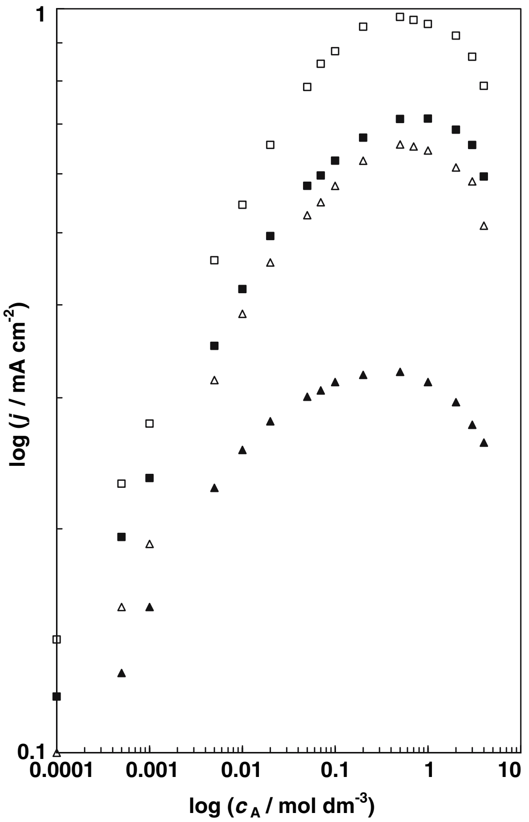

Fig. 5 Dependence of the current density on the amine concentrations in 0.1 mol dm^{-3} NaOH at $E = –0.2$ V versus SCE for (■) 2-aminoethanol and (□) 2-amino-1-butanol and at $E = –0.15$ V versus SCE for (▲) 2-aminoethanol and (△) 2-amino-1-butanol. dE/dt = 0.1 V s^{-1}

alcoholamine concentration increases, (see Figs. 3, 4). This shift is typical of reactions involving adsorbed molecules. Stronger interactions between the organic molecules and the electrode surface may account for the increase in current density with increasing carbon chain length in the alcoholamine molecules.

The influence of the competitive adsorption of alcoholamine and hydroxyl ions was verified in experiments in which the concentration of one component was kept constant while that of the other was varied. The plots of the logarithm of current density versus the logarithm of substrate and supporting electrolyte concentration at constant electrode potentials are depicted in Figs. 5 and 6, respectively. The slopes of the straight lines of the appropriate log *j* - log *c* relationships give the reaction order with respect to substrate concentration, $z_{\mathrm{A}} = \mathrm{d}j/\mathrm{d}c_{\mathrm{A}}$ and to hydroxyl anion concentration, $z_{\mathrm{OH}^-} = \mathrm{d}j/\mathrm{d}c_{\mathrm{OH}^-}$, respectively.

The resulting z_{A} is 0.29 ± 0.03 and 0.30 ± 0.01 for $c_{\mathrm{A}} \leq 0.01$ mol dm^{-3} of ethanolamine and butanolamine, respectively. For $c_{\mathrm{OH}^-} \leq 0.1$ mol dm^{-3} the z_{OH^-} is 0.28 ± 0.01 and 0.3 ± 0.01 for 0.001 mol dm^{-3} of ethanolamine and butanolamine, respectively. When the concentration of alcoholamine increases to 0.01 mol dm^{-3} the resulting z_{OH^-} is 0.26 ± 0.02 and 0.24 ± 0.03, respectively. The fractional reaction order gives clear evidence that the kinetics of alcoholamine oxidation are influenced by the relative surface concentration of organic species and hydroxyl anions. The reaction rate decreases after passing a maximum when the amount of either organic molecules or OH$^-$ prevails at the electrode/solution interface (see Figs. 5, 6).

In order to obtain information on the rate determining step of alcoholamine oxidation, Tafel analyses of voltammograms were made. The slopes, $\mathrm{d}E/\mathrm{d}\log j = 2.303RT/\alpha nF$ for the linear parts of plots in log *j*–*E* coordinates (Fig. 7) give values of 0.175 ± 0.020 and 0.200 ± 0.020 V per decade of current density for the lowest concentration of ethanolamine and butanolamine, respectively. The d*E*/log *j* slopes increase somewhat with increasing alcoholamine content. Moreover, fairly similar Tafel slopes were obtained for pH in the range 11–13.7. The average electron transfer coefficient, αn = 0.30 ± 0.03 derived from the Tafel slopes, lower than 0.5, is compatible with the assumption of an adsorption step preceding the first electron transfer step determining the overall reaction rate. Further steps proceed so fast that they have no influence on the rate. As follows from the kinetic theory of electrode reaction, in the case of a simple rate determining step with no contribution of adsorption, a Tafel slope of only 0.12 V decade^{-1} should be found [53].

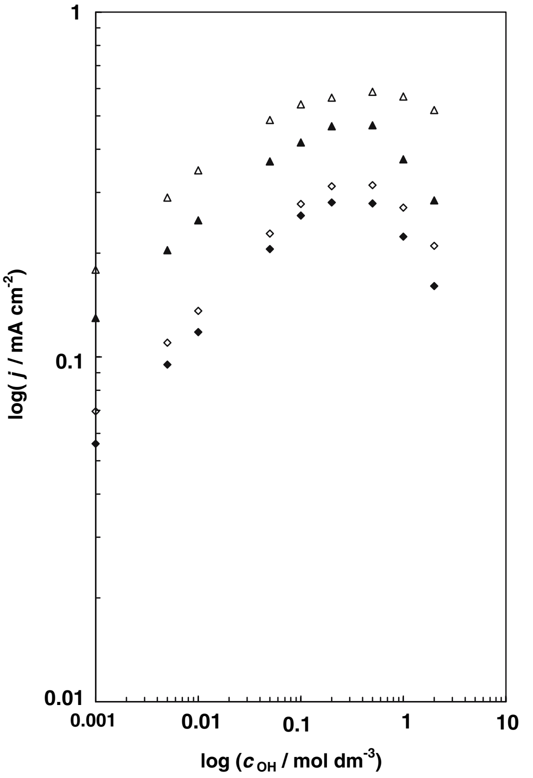

Fig. 6 Dependence of current density on the NaOH concentrations at *E* = –0.15 V versus SCE in 0.001 mol dm^{-3} (♦) 2-aminoethanol and (◇) 2-amino–1-butanol and in 0.01 mol dm^{-3} (▲) 2-aminoethanol and (Δ) 2-amino-1-butanol. d*E*/d*t* = 0.1 V s^{-1}

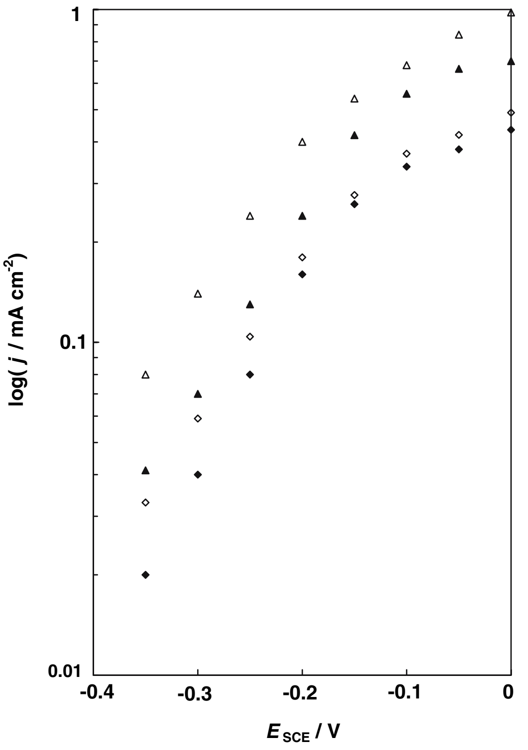

Fig. 7 Dependence of current density on gold electrode potential in 0.1 mol dm^{-3} NaOH for: 0.001 mol dm^{-3} (♦) 2-aminoethanol and (◇) 2-amino-1-butanol and for 0.01 mol dm^{-3} (▲) 2-aminoethanol and (Δ) 2-amino-1-butanol. d*E*/d*t* = 0.1 V s^{-1}

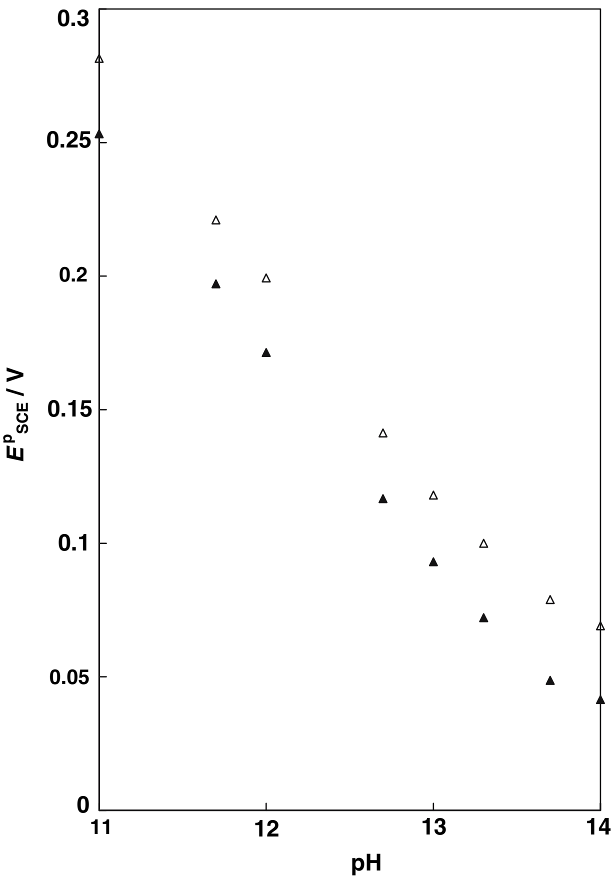

Fig. 8 Dependence of peak potential on pH of the supporting electrolyte solution for 0.01 mol dm^{-3}: (▲)2-aminoethanol and (Δ) 2-amino-1-butanol

Finally, analysis of the variation of the peak potential E_p with pH of supporting electrolyte shows that during the electrode process not only electrons but also protons are released from the organic molecules. The peak potentials shift linearly to less positive potentials with increasing pH. For the amines studied in the pH range between 11 and 13 the E_p versus pH plots (Fig. 8) are linear with an average slope of –82 ± 2 mV per unit pH. The slope suggests the participation of unequal numbers of protons and electrons in the electrooxidation reaction.

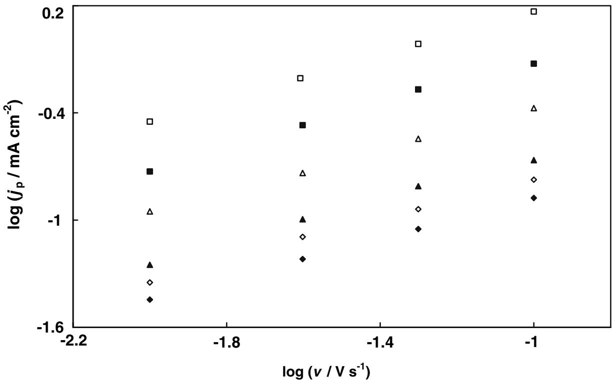

Fig. 9 Logarithm of peak current density versus the logarithm of potential sweep rate for 2-aminoethanol of (♦) 0.0005 mol dm^{-3}; (▲) 0.001 mol dm^{-3}; and (■) 0.005 mol dm^{-3} and for 2-amino-1-butanol of (◇) 0.0005 mol dm^{-3}; (Δ) 0.001 mol dm^{-3}; (□) 0.005 mol dm^{-3} on gold electrode in 0.1 mol dm^{-3} NaOH

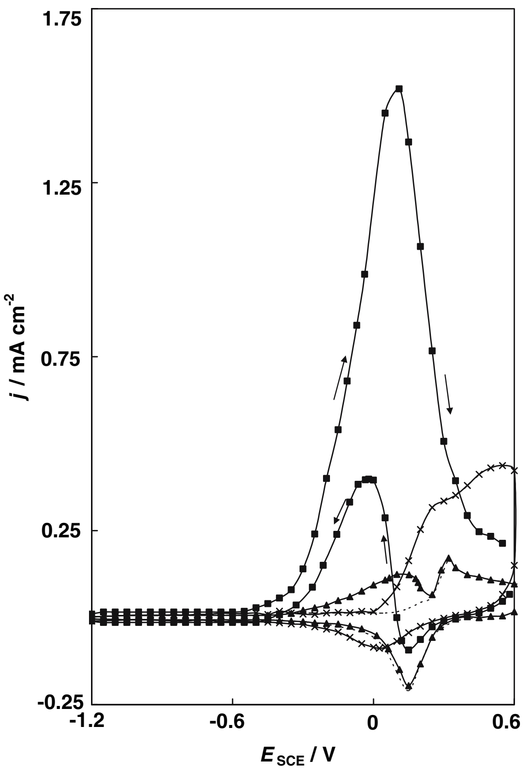

Fig. 10 Cyclic voltammograms of the gold electrode in 0.1 mol dm^{-3} NaOH (dotted line) and with 0.01 mol dm^{-3}: (■) 2-amino-1-butanol; (×) butylamine and (▲) 1-butanol. d*E*/d*t* = 0.1 V s^{-1}

For both alcoholamines studied the oxidation peak potential shifts positively with increasing sweep rate, confirming the irreversibility of the electrocatalytic process. The log j_p versus log v plots, (Fig. 9) are linear with an average slope of $d\log j_p/d\log v \approx 0.6$. The magnitude of this parameter means that the mechanism of alcoholamine oxidation on gold is not pure from the kinetic point of view and may indicate a mixed, i.e., diffusion–adsorption rate control, as for a pure diffusion process the value of slope should be 0.5, while for a pure adsorption controlled process it should be 1.

It is interesting to compare the voltammetric response of a gold electrode in the presence of aliphatic alcoholamines, alcohols and amines. Figure 10 reveals clear differences between the electrooxidation activity of butanolamine, butylamine and butanol as examples. As follows from both *j*–*E* curves presented in Fig. 10 and from literature data [45, 46], aliphatic amines are inactive at gold electrode potentials below $E \approx 0$ V. Their oxidation proceeds irreversibly only in parallel with gold oxide formation. When comparing the response of the gold electrode in the supporting electrolyte solution with those obtained in the presence of amine, the charge used for reduction of gold oxide in the presence of amine is smaller than that in the solution without solute. This points to participation of gold oxide in the oxidation reaction of amines. The electrooxidation of butanol starts at about –0.35 V, when the surface is partially covered with adsorbed hydroxyl ions [4, 8]. Earlier studies have shown that the presence of hydroxide species on the electrode surface is the precondition for the oxidation of aliphatic alcohols on gold [4, 12]. The kinetic parameters (Tafel slope, reaction order with respect to both substrate and hydroxyl anion concentration) obtained for alcoholamines are very close to those evaluated for aliphatic amines [45, 46]. Two major factors are important in evaluation of the catalytic effect of electrodes on electrooxidation processes: decrease in overpotential of oxidation and increase in current density as compared with the bare electrode. In this context, the highest catalytic effect of the gold electrode on electrooxidation of the compounds studied is achieved for butanolamine. It should be noted that its oxidation starts at potentials even more negative than that of the onset of alcohol electrooxidation. Moreover, the current density of butanolamine oxidation is about twelve and three times greater than those observed for butanol and butylamine, respectively. There is no doubt that the presence of the second electron donating group (–OH group), besides the –NH_2 group, in the alcoholamine molecule must be responsible for such differences in the activity of this class of compounds at the gold/solution interface. Taking into account the potential ranges in which alcoholamines, amines and alcohols are oxidized it can be assumed that in the alcoholamine molecule the CH_2OH group is oxidized first and only after that the NH_2 group.

In the light of the results, the possible reaction pathways for alcoholamine electrooxidation on gold in alkaline solution can be proposed as shown in Scheme 1.

The first step in the proposed mechanism is the formation of the catalytic $AuOH_{ad}^{\delta-}$ layer at the electrode surface. Next, the adsorption of alcoholamine is followed by hydrogen abstraction from the alcoholamine molecule via a transient adsorbate complex formed as a result of the interaction between adsorbed substrate molecules and the $AuOH_{ad}^{\delta-}$ catalytic sites. The heterogeneous dehydrogenation of the alcoholamine molecule, involving electron

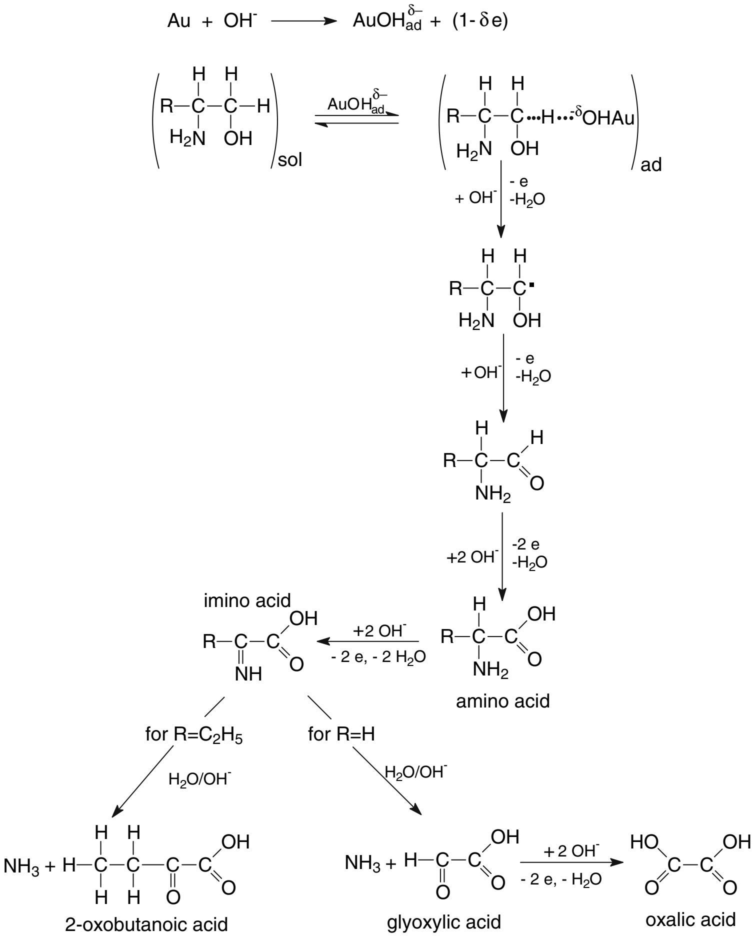

Scheme 1 Possible reaction pathways for electrooxidation of alcoholamines on a gold electrode in an alkaline solution

transfer to the gold electrode and the formation of water molecules determines the rate of the whole process. Further steps proceed so fast that they have no influence on the rate of alcoholamine oxidation. It should be emphasized that alcoholamine molecules may be adsorbed on the gold catalyst surface without being involved in the oxidation reaction; in particular at small coverages of the metal surface with preadsorbed hydroxyl ions at low anodic potentials they may actually inhibit adsorption of further hydroxyl ions by blocking the electrode surface. This would account for the observed decrease in the rate of alcoholamine oxidation at high concentration. This effect, as well as the analogous decrease in the reaction rate observed at high hydroxyl ions concentration, are indicative of the competitive adsorption of alcoholamine molecules and hydroxyl ions at gold. As a result of the CH_2OH group oxidation in alcoholamine the respective amino acid may be formed, which is then oxidized to different final products depending on the order of the carbon atom to which the amino group in the substrate molecule is attached. For ethanolamine with the NH_2 group linked to the first ordered C-atom, the final product should be oxalic acid (dicarboxylic acid), while 2-oxobutanoic acid (keto acid) should be the final product of butanolamine oxidation, in which the NH_2 group is associated with the second ordered C-atom. Differences in the adsorption properties of alcoholamines may account for the observed increase in the oxidation rate for ethanolamine and butanolamine, respectively.

Acknowledgements Financial support of this work by the Ministry of Scientific Research and Information Technology, Poland, is gratefully acknowledged. The author thanks Professor M. Bełtowska-Brzezinska for valuable discussion.

References

1. Bełtowska-Brzezinska M, Vielstich W (1977) Electrochim Acta 22:1313
2. Bełtowska-Brzezinska M (1979) Electrochim Acta 24:409
3. Bełtowska-Brzezinska M (1980) Electrochim Acta 25:267
4. Bełtowska-Brzezinska M (1980) Kinetics and mechanism of electrocatalytic oxidation of alcohols on gold, platinum and gold-platinum alloys. UAM Press, Poznań
5. Beden B, Cetin I, Kahyaoglu A, Takky D, Lamy C (1987) J Catal 104:37
6. Holze R, Łuczak T, Bełtowska-Brzezinska M (1990) Electrochim Acta 35:1345
7. Beden B, Leger JM, Lamy C (1992) In: Bockris JO'M, Conway BE, White RE (eds) Modern aspects of electrochemistry, vol 22. Plenum Press, New York, p 97–265 and references therein
8. Łuczak T, Bełtowska-Brzezinska M, Holze R (1993) J Appl Electrochem 3:1039
9. Holze R, Łuczak T, Bełtowska-Brzezinska M (1994) Electrochim Acta 39:485
10. Holze R, Łuczak T, Bełtowska-Brzezinska M (1994) Electrochim Acta 39:991
11. Łuczak T, Holze R, Bełtowska-Brzezinska M (1994) Electroanalysis 6:773
12. Bełtowska-Brzezinska M, Łuczak T, Holze R (1997) J Appl Electrochem 27:999
13. Bełtowska-Brzezinska M, Łuczak T (2001) Electroanalysis 15:1270
14. Raichewa SN, Kalcheva SV, Christov MV, Sokolova EI (1974) J Electroanal Chem 55:213
15. Parsons R, VanderNoot T (1988) J Electroanal Chem 257:9
16. Wieckowski A (1975) J Electrochem Soc 122:252
17. Bełtowska-Brzezinska M, Dutkiewicz E, Skołuda P (1984) J Electroanal Chem 181:235
18. Bełtowska-Brzezinska M, Heitbaum J (1985) J Electroanal Chem 183:167
19. Holze R, Bełtowska-Brzezinska M (1986) J Electroanal Chem. 201:387
20. Lipkowski J, Stolberg L (1992) In: Lipkowski J, Ross PN (eds) Adsorption of molecules at metal electrodes, vol 1, Wiley-VCH, New York
21. Trasatti S (1992) Electrochim Acta 37:2137
22. Łuczak T, Bełtowska-Brzezinska M, Holze R (1993) Electrochim Acta 38:717
23. Bełtowska-Brzezinska M, Łuczak T, Holze R (1998) Surf Sci 418:281
24. Hauffe W, Heitbaum J (1978) Ber Bunsenges Phys Chem 82:487
25. Takky D, Beden B, Léger JM, Lamy C (1983) J Electroanal Chem. 145:461
26. Desilvestro J, Weaver MJ (1986) J Electroanal Chem 209:377
27. Ocon P, Alonso C, Celdran R, Gonzales-Velasko J (1986) J Electroanal Chem 206:179
28. Burke LD, Lee BH (1992) J Electroanal Chem 330:637
29. Burke LD, Buckley DT, Morrissey JA (1994) Analyst 119:841
30. Burke LD, Moran JM, Nugent PF (2003) J Solid State Electrochem 7:529
31. Mann CK (1964) Anal Chem 36:2424
32. Barnes KK, Mann CK (1967) J Org Chem 32:1474
33. Horányi G, Rizmayer EM (1988) J Electroanal Chem 251:403
34. Horányi G, Rizmayer EM (1989) J Electroanal Chem 264:273
35. Huerta F, Morallón E, Quijada C, Vázquez JL, Pérez JM, Aldaz A (1999) J Electroanal Chem 467:105
36. Huerta F, Morallón E, Pérez JM, Vázquez JL, Aldaz A (1999) J Electroanal Chem 469:159
37. Luo P, Zhang F, Baldwin RP (1991) Anal Chim Acta 244:169
38. Jackson WA, Lacourse WR, Dobberpuhl DA, Johnson DC (1991) Electroanalysis 3:607
39. Dobberpuhl DA, Johnson DC (1995) Anal Chem 67:1254
40. Dobberpuhl DA, Johnson DC (1996) Electroanalysis 8–9:726
41. Łuczak T (2005) Collect Czech Chem Commun 70:2027
42. Łuczak T (2005) Annals of the polish chemical society 666
43. Łuczak T (2006) Colloids Surf A 280:125
44. Łuczak T (2006) Asian Chem Lett 10:25
45. Łuczak T (2006) Collect Czech Chem Commun 71:1371
46. Łuczak T (2007) J Appl Electrochem 37:269
47. Will FG, Hess HJ (1973) J Electrochem Soc 120:1
48. Will FG (1986) J Electrochem Soc 133:454
49. Angerstein-Kozlowska H, Conway BE, Burnett B, Mozota J (1979) J Electroanal Chem 100:417
50. Adzić RR, Markocić NM, Vesović VB (1986) J Electroanal Chem 165:532
51. Alonso C, Gonzáles-Velasco J (1988) J Electroanal Chem 248:193
52. Newman RC, Burstein GT (1981) J Electroanal Chem 129:343
53. Kisza A (2001) Electrochemistry II. WNT, Warsaw, p 94